研究成果の刊行に関する一覧表

雑誌

発表者氏名	論文タイトル名	発表雑誌名	巻号	ページ	出版年
Fukuma, M.	Up-regulation of Id2, an oncogenic helix-loop-helix protein, is mediated by the chimeric EWS/ets protein in Ewing sarcoma.	Oncogene	22・1	1-9	2003
Ochi, K.	The use of isolated mature osteoblasts in abundance acts as desired-shaped bone regeneration in combination with a modified poly DL-lactic- co-glycolic acid (PLGA)-collagen sponge.	J. Cell. Physiol.	194	45-53	2003
Shibata, R.	Responsiveness of chemotherapy based on the histological type and WT1 mutation in bilateral Wilms tumor.	Pathology international	53	214-220	2003
Shibata, R.	Primary carcinosarcoma of the vagina.	Pathology Int.	53	106-110	2003
Taguchi T, Fujimoto J, et al.	Pre-BCR-mediated signal inhibits CD24-induced apoptosis in human pre-B cells.	J-Immunol	170(1)	252-60	2003
Mori T, Fujimoto J, et al.	Anaplastic large cell lymphoma in Japanese children: Retrospective analysis of 34 patients diagnosed at the National Research Institute for Child Health and Development.	Br-J-Haematol	121(1)	94-6	2003
Mimori K, Fujimoto J, et al.	Co-stimulatory signals distinctively affect CD20- and B-cell-antigen-receptor-mediated apoptosis in Burkitt's lymphoma /leukemia cells.	Leukemia	17(6)	1164-74	2003
Furusawa T, Fujimoto J, et al.	Catalytic RAG1 mutants obstruct V(D)J recombination in vitro and in vivo.	Mol Immunol	39(14)	871-8	2003

研究成果の刊行に関する一覧表

雑誌

発表者氏名	論文タイトル名	発表雑誌名	巻号	ページ	出版年
Ohkoshi K, Fujimoto J, et al.	In vitro oocyte culture and somatic cell nuclear transfer used to produce a live-born cloned goat.	Cloning-Stem-Cells	5(2)	109-15	2003

研究成果の刊行に関する一覧表

雑誌

発表者氏名	論文タイトル名	発表雑誌名	巻号	ページ	出版年
Ohtsuka M, Komuro I, et al.	Role of Na^+-Ca^{2+} exchanger in myocardial ischemia/reperfusion injury: evaluation using a heterozygous Na^+-Ca^{2+} exchanger knockout mouse model.	Biochem Biophys Res Commun	314	849-853	2004
Miyauchi H, Komuro I, et al.	Akt negatively regulates the in vitro lifespan of human endothelial cells via a p53/p21-dependent pathway.	EMBO J	23	212-220	2004
Matsuura K, Komuro I, et al.	Adult cardiac Sca-1 positive cells differentiate into beating cardiomyocytes.	J Biol Chem	279	11384-11391	2004
Ohsawa Y, Komuro I, et al.	Overexpression of P104L mutant caveolin-3 in mice develops hypertrophic cardiomyopathy with enhanced contractility in association with increased endothelial nitric oxide synthase activity.	Hum Mol Genet	13	151-157	2004
Ohtsuka M, Komuro I, et al.	Cytokine therapy prevents left ventricular remodeling and dysfunction after myocardial infarction through neovascularization.	FASEB J	18	851-853	2004
Toko H, Komuro I, et al.	Angiotensin II Type 1a Receptor Is Involved in Cell Infiltration, Cytokine Production, and Neovascularization in Infarcted Myocardium.	Arterioscler Thromb Vasc Biol	24	664-670	2004
Akazawa H, Komuro I, et al.	A novel LIM protein Cal promotes cardiac differentiation by association with CSX/NKX2-5.	J Cell Biol	164	395-405	2004

研究成果の刊行に関する一覧表

雑誌

発表者氏名	論文タイトル名	発表雑誌名	巻号	ページ	出版年
Kasai H, Komuro I, et al.	Direct measurement of Ca^{2+} concentration in the SR of living cardiac myocytes.	Biochem Biophys Res Commun	314	1014-1020	2004
Zou Y, Komuro I, et al.	Mechanical stress activates angiotensin II type 1 receptor without the involvement of angiotensin II.	Nat Cell Biol	6	499-506	2004
Ogihara T, Komuro I, et al.	Oxidative stress induces insulin resistance by activating the nuclear factor-kappaB pathway and disrupting normal subcellular distribution of phosphatidylinositol 3-kinase.	Diabetologia	47	794-805	2004
Minamino T, Komuro I, et al.	The role of vascular cell senescence in atherosclerosis: antisenescence as a novel therapeutic strategy for vascular aging.	Curr Vasc Pharmacol	2	141-148	2004
Funabashi N, Komuro I, et al.	Images in cardiovascular medicine. Double aortic arch with a compressed trachea demonstrated by multislice computed tomography.	Circulation	110	e68-e69	2004
Hayashi D, Komuro I, et al.	Atrial natriuretic peptide inhibits cardiomyocyte hypertrophy through mitogen-activated protein kinase phosphatase-1.	Biochem Biophys Res Commun	322	310-319	2004
Funabashi N, Komuro I, et al.	New method of measuring coronary diameter by electron-beam computed tomographic angiography using adjusted thresholds determined by calibration with aortic opacity.	Circ J	68	769-777	2004

研究成果の刊行に関する一覧表

雑誌

発表者氏名	論文タイトル名	発表雑誌名	巻号	ページ	出版年
Akazawa H, Komuro I, et al.	Diphtheria toxin-induced autophagic cardiomyocyte death plays a pathogenic role in mouse model of heart failure.	J Biol Chem	279	41095-41103	2004
Ikeda Y, Komuro I, et al.	Vasorin, a transforming growth factor beta-binding protein expressed in vascular smooth muscle cells, modulates the arterial response to injury in vivo.	Proc Natl Acad Sci U S A	101	10732-10737	2004
Matsuura K, Komuro I, et al.	Cardiomyocytes fuse with surrounding non-cardiomyocyres and re-enter the cell cycle.	J Cell Biol	167	351-363	2004
Naito, A.T, Komuro I, et al.	Steroid-responsive thromboangiitis obliterans.	Lancet	364	1098	2004
Iwanaga K, Komuro I, et al.	Effects of G-CSF on cardiac remodeling after acute myocardial infarction in swine.	Biochem Biophys Res Commun	325	1353-1359	2004
Iwamoto T, Komuro I, et al.	Salt-sensitive hypertension is triggered by Ca(2+) entry via Na(+)/Ca(2+) exchanger type-1 in vascular smooth muscle.	Nat Med	10	1193-1199	2004
Minamino T, Komuro I, et al.	The role of vascular cell senescence in atherosclerosis: antisenescence as a novel therapeutic strategy for vascular aging.	Curr Vasc Pharmacol	2	141-148	2004
Minamino T, Komuro I, et al.	Vascular cell senescence and vascular aging.	J Mol Cell Cardiol	36	175-183	2004
Minamino T, Komuro I, et al.	Akt-induced Cellular Senescence: Implication for Human Disease.	Cell Cycle	3	449-451	2004
Komuro I, Ohtsuka M.	Forefront of Na+/Ca2+ exchanger studies: role of Na+/Ca2+ exchanger--lessons from knockout mice.	J Pharmacol Sci	96	23-26	2004

研究成果の刊行に関する一覧表

雑誌

発表者氏名	論文タイトル名	発表雑誌名	巻号	ページ	出版年
Harada M, Komuro I, et al.	G-CSF prevents cardiac Remodeling after myocardial infarction by activating Jak/Stat in cardiomyocytes.	Nat Med	11	305-311	2005
Tsuchiya, K., Mori, T., Chen, G., Ushida, T., Tateishi, T., Matsuno, T., Sakamoto, M., and Umezawa, A (Correspondence to A.U.)	Custom-shaping system for bone regeneration by seeding marrow stromal cells onto a web-like biodegradable hybrid sheet.	Cell Tissue Res,	316	141-153	2004
Sakurai, K., Iizuka, S., Shen, J-S., Meng, X-L., Mori, T., Umezawa, A., Ohashi, T., and Eto, Y.	Brain transplantation of genetically modified bone marrow stromal cells corrects CNS pathology and cognitive function in MPS VII mice.	Gene Therapy,	11(19)	1475-1481	2004
Oikawa, K., Ohbayashi, T., Kiyono, T., Nishi, H., Isaka, K., Umezawa, A., Kuroda, M., and Mukai, K.	Expression of a Novel Human Gene, Human Wings Apart-Like (hWAPL), Is Associated with Cervical Carcinogenesis and Tumor Progression.	Cancer Res,	64	3545-3549	2004
Takeda, Y., Mori, T., Imabayashi, H., Kiyono, T., Gojo, S., Miyoshi, S., Ita, M., Segawa, K., Ogawa, S., Sakamoto, M., Nakamura, S., and Umezawa, A. (Correspondence to A.U.)	"Can the life-span of human marrow stromal cells be prolonged by bmi-1, E6, E7, and/or telomerase without affecting cardiomyogenic differentiation?",	J Gene Med	6(8)	833-845	2004
Higuchi, A., Hamamura, A., Shindo, Y., Kitamura, H., Yoon, B-O., Mori, T., Uyama, T., and Umezawa, A.	Photon-modulated changes of cell attachments on poly(spiropyran-co-methylmethacrylate) membranes,	Biomacromolecules	5(5)	1770-1774	2004

研究成果の刊行に関する一覧表

雑誌

発表者氏名	論文タイトル名	発表雑誌名	巻号	ページ	出版年
Kiyokawa N, Sekino T, Matsui T, Takenouchi H, Mimori K, Tang W, Matsui J, Taguchi T, Katagiri YU, Okita H, Matsuo Y, Karasuyama H, Fujimoto J.	Diagnostic Importance of CD179a/b as Markers of Precursor B-Cell Lymphoblastic Lymphoma.	Modern Pathol	17	423-429	2004
Takenouchi H, Kiyokawa N, Taguchi T, Matsui J, Katagiri YU, Okita H, Okuda K, Fujimoto J.	Shiga toxin binding to globotriaosyl ceramide induces intracellular signals that mediate cytoskeleton remodeling in human renal carcinoma-derived cells.	J Cell Sci	117	3911-3922	2004
Tang W, Kiyokawa N, Eguchi T, Matsui J, Takenouchi H, Honma D, Yasue H, Enosawa S, Mimori K, Itagaki M, Taguchi T, Katagiri YU, Okita H, Amemiya H, Fujimoto J.	Development of novel monoclonal antibody 4G8 against swine leukocyte antigen class I a chain.	Hybrid Hybridomics	23	187-191	2004
Taguchi T, Kiyokawa N, Takenouchi H, Matsui J, Tang W, Nakajima H, Suzuki K, Shiozawa Y, Saito M, Katagiri YU, Takahshi T, Karasuyama H, Matsuo Y, Okita H, Fujimoto J.	Deficiency of BLNK hampers PLC-g2 phosphorylation and Ca2+ influx induced by the pre-B cell receptor in human pre-B cells.	Immunology	112	575-582	2004

研究成果の刊行に関する一覧表

雑誌

発表者氏名	論文タイトル名	発表雑誌名	巻号	ページ	出版年
Tang W-R, Shioya N, Eguchi T, Ebata T, Matsui J, Takenouchi H, Honma D, Yasue H, Takagaki Y, Enosawa S, Itagaki M, Taguchi T, Kiyokawa N, Amemiya H, Fuijmoto J.	Characterization of new monoclonal antibodies against porcine lymphocytes: molecular characterization of clone 7G3, an antibody reactive with the constant region of the T-cell receptor d-chains.	Veterinary Immunol Immunopathol	103	113-127	2005

ACADEMIC PRESS

Available online at www.sciencedirect.com

SCIENCE DIRECT®

Biochemical and Biophysical Research Communications 305 (2003) 806–810

BBRC

www.elsevier.com/locate/ybbrc

Cdc42 plays a critical role in assembly of sarcomere units in series of cardiac myocytes

Toshio Nagai,[a] Mariko Tanaka-Ishikawa,[b] Ryuichi Aikawa,[b] Hisamitsu Ishihara,[c] Weidung Zhu,[b] Yoshio Yazaki,[d] Ryozo Nagai,[b] and Issei Komuro[a,*]

[a] *Department of Cardiovascular Science and Medicine, Chiba University Graduate School of Medicine, 1-8-1 Inohana, Chuo-ku, Chiba 260-8670, Japan*
[b] *Department of Cardiovascular Medicine, University of Tokyo Graduate School of Medicine, Tokyo, Japan*
[c] *Department of Internal Medicine, Tohoku University School of Medicine, Sendai, Japan*
[d] *International Medical Center of Japan, Tokyo, Japan*

Received 21 April 2003

Abstract

Cardiomyocyte hypertrophy is observed in various cardiovascular diseases and causes heart failure. We here examined the role of small GTP-binding proteins of Rho family in phenylephrine (PE)-or leukocyte inhibitory factor (LIF)-induced hypertrophic morphogenesis of cultured neonatal rat cardiomyocytes. Both LIF and PE increased cell size of cardiomyocytes. LIF induced an increase in the length/width ratio of cardiomyocytes, while PE did not change the ratio. Adenoviral gene transfer of constitutively active mutants of Cdc42 increased the length/width ratio of cardiomyocytes and dominant negative mutants of Cdc42 conversely inhibited LIF-induced cell-elongation, while mutants of RhoA and Rac1 did not affect the length/width ratio of cardiomyocytes. These results suggest that Cdc42, but not RhoA and Rac1, is involved in LIF-induced sarcomere assembly in series in cardiomyocytes.

Keywords: RhoA; Rac1; Cdc42; Leukocyte inhibitory factor; Cardiac hypertrophy

One of the distinct features of cardiomyocyte hypertrophy is the assembly of contractile proteins into organized sarcomeric units. Immunocytochemical studies have revealed the process of sarcomere assembly (myofibrillogenesis) in cultured myocytes and developing chicken heart [1]. The morphological phenotypes of ventricular myocytes are different among physiological, concentric, and eccentric hypertrophy [2]. Physiological hypertrophy is characterized by proportional increases in width and length of cardiomyocytes. Concentric hypertrophy is induced by pressure overload and characterized by more increase in width than length while eccentric hypertrophy is induced by volume overload and characterized by more increase in length of cardiomyocytes. Many growth factors induce cardiomyocyte hypertrophy in vitro with distinctive features through various intracellular signaling pathways [3–6]. Concentric hypertrophy is induced by mechanical stretch and agonists of Gq protein-coupled receptors such as phenylephrine (PE), angiotensinII (AngII), and endothelin-1 [4]. In contrast, gp130 ligands such as cardiotrophin-1 (CT-1) or leukocyte inhibitory factor (LIF) induced cardiomyocyte hypertrophy with an increase in rather cell length than width and this feature of cardiomyocytes resembles that of eccentric hypertrophy [5].

Small molecular weight GTP-binding proteins (small G-proteins) of Rho family including RhoA, Rac1, and Cdc42 play critical roles in cell shape, adhesion, and motility in various types of cells [7–10]. In cardiomyocytes, RhoA, and Rac1 are involved in AngII- and PE-induced cardiac hypertrophy [11,12]. In this study, we examined the roles of small G-proteins of Rho family in PE- or LIF-induced sarcomere assembly of cardiac myocytes using adenovirus-mediated gene expression system. We here report that among RhoA, Rac1, and Cdc42, only Cdc42 is involved in LIF-induced myofibril elongation.

* Corresponding author. Fax: +81-43-226-2557.
E-mail address: komuro-tky@umin.ac.jp (I. Komuro).

0006-291X/03/$ - see front matter © 2003 Elsevier Science (USA). All rights reserved.
doi:10.1016/S0006-291X(03)00838-6

Materials and methods

Antibodies and reagents. Monoclonal anti-myc antibody (9E10) and monoclonal anti-cardiac myosin heavy chain antibody (MF20) were prepared from American Type Culture Collection. TRITC-labeled phalloidin and phenylephrine were purchased form Sigma–Aldrich Japan, rhodamine conjugated anti-mouse IgG was from Chemicon, and FITC conjugated goat anti-mouse IgG was from American Qualex. LIF was purchased from Chemicon.

Cell culture. Primary cultures of cardiac ventricular myocytes from 1-day-old Wistar rats were obtained as described previously [13]. Cells were plated at a field density of 1×10^5cells/cm^2 on either collagen-coated 35-mm culture dishes or coverslips with 2 ml of Dulbecco's modified Eagle's medium with 10% fetal bovine serum. Culture media were changed to serum-free media after 24 h. Myocytes were further cultured under serum-free conditions for 24 h and then treated with either 10^{-9} M LIF or 10^{-5} M PE for 48 h.

Recombinant adenovirus vector and adenoviral gene transfer. Six types of E1-deleted, replication deficient adenovirus vectors expressing myc-epitope tagged constitutively active or dominant negative recombinant cDNA of Rho family were used. Adenoviruses encoding C.A.RhoA (RhoA V14), D.N.RhoA (RhoA N19), C.A.Rac1 (Rac1 V12), and D.N.Rac1 (Rac1 N17), C.A.Cdc42 (Cdc42 V12), and D.N.cdc42 (Cdc42 N17) were prepared. Adenovirus vector containing the LacZ gene was used as a control vector. Cardiomyocytes were infected with recombinant adenoviruses at a multiplicity of infection (MOI) of 50 U in 0.5 ml DMEM for 1 h at 37 °C in humidified 5% CO_2 incubator and further cultured in serum-free DMEM for 48 h. The expression of RhoA, Rac1, and Cdc42 was confirmed by Western blotting using antibodies specific for Rho, Rac1, and Cdc42 (data not shown). Efficiency of gene transfer into cardiomyocytes was assessed by X-gal staining [14]. More than 95% of cardiomyocytes exhibited LacZ-positive staining (data not shown).

Immunofluorescent cytochemistry. Immunostaining to examine the morphology of cardiomyocytes was performed as described previously [15]. Briefly, cells were fixed in 3% paraformaldehyde for 10 min, treated with 50 mM NH_4Cl, and permeabilized with 0.1% Triton X-100 and 5% fetal bovine serum for 30 min at 37 °C. The samples were incubated with either anti-myc antibody (9E10) to assess adenoviral mediated gene expression or anti-cardiac myosin heavy chain antibody (MF20) to examine myofibrils followed with FITC-conjugated anti-mouse IgG second antibody and TRITC-labeled phalloidin.

To assess the hypertrophic phenotype of cardiomyocytes, cell length and width were measured and length/width ratio was calculated. Definitions of morphometric parameters were as previously described [5]. Cell length was defined as the maximum longitudinal extension of individual cells. Maximum cell width was measured perpendicular to the axis defining cell length. These parameters were measured with graphic analyzing software, IP lab on the digital images taken by CCD camera on the fluorescent microscope. More than 100 cells on every dish were measured.

Statistics. All results (means ± SE) were obtained from three independent experiments. Statistical comparison of the control group with treated groups was carried out with 1-way ANOVA and Dunnett's t test. The accepted level of significance was $p < 0.05$. More than 100 cardiomyocytes were examined in each experiment.

Results and discussion

Role of small G-proteins of Rho family in sarcomeric organization

To investigate the role of small G-proteins RhoA, Rac1, and Cdc42 in sarcomeric organization in cultured

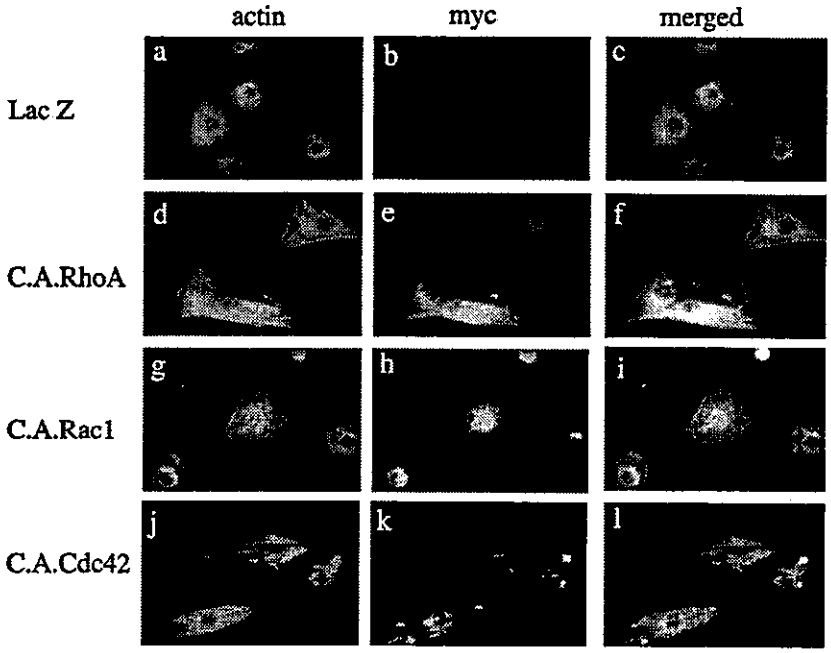

Fig. 1. Constitutively active mutants of Rho family proteins induce sarcomeric organization in cardiomyocytes. Cardiomyocytes were infected with adenovirus constructs containing LacZ without myc tag (a–c), constitutively active mutants of RhoA (d–f), Rac1 (g–i), and Cdc42 (j–l) for 48 h and then stained with anti-myc monoclonal antibody (9E10) followed by FITC-conjugated anti-mouse immunoglobulin (green) and TRITC-labeled phalloidin for actin (red).

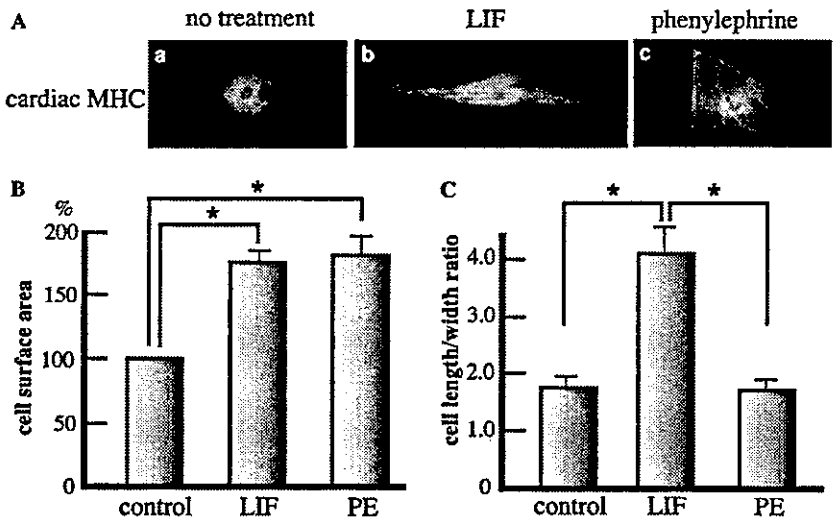

Fig. 2. Effects of LIF and PE on cell-length/width ratio and cell surface area. (A) Cardiomocytes were untreated (a) or treated with 10^{-9} M LIF (b) or 10^{-5} M PE (c) for 48 h and stained with anti-cardiac myosin heavy chain antibody (MF20) followed by FITC-conjugated anti-mouse immunoglobulin. (B) In each experiment, the cell surface area of over 100 cardiomyocytes was measured. The data represent the mean percentage of controls (100%) from three independent experiments (means ± SE). $^{*}p < 0.01$ vs control. (C) Cell-length/width ratio of over 100 cardiomyocytes was quantitatively examined in each experiment. The results are from three independent experiments (means ± SE). $^{*}p < 0.05$ vs control and $^{**}p < 0.05$ vs control treated with LIF.

cardiac myocytes, cells were infected with adenovirus encoding C.A. mutant of RhoA, Rac1, or Cdc42. Immunocytochemical staining revealed that each of the three types of mutant induced sarcomeric organization in infected cells (Fig. 1). When cardiomyocytes were incubated with either LIF or PE for 48 h, clear striated bands reflecting sarcomere were observed (Figs. 2A b,c) and the cell size was increased (control 100% vs LIF 175%, $p < 0.01$; control 100% vs PE 180%, $p < 0.01$, Fig. 2B). However, there was considerable difference in cell shape between LIF- and PE-treated cardiomyocytes. LIF induced an increase in the length/width ratio, leading to the elongated cell shape, while PE did not change the ratio (Figs. 2A b, c, and C).

Role of small G-proteins of Rho family in morphological change

Overexpression of D.N.RhoA, D.N.Rac1, or D.N.Cdc42 inhibited LIF- and PE-induced sarcomere assembly (Fig. 3). Although overexpression of D.N. RhoA or D.N. Rac1 had no effect on LIF-induced cell elongation, D.N.Cdc42 inhibited sarcomere organization in series (Fig. 3). D.N.Cdc42 significantly reduced the length/width ratio of LIF-treated cardiomyocytes but neither D.N.RhoA nor D.N.Rac1 had the effect on the length/width ratio (Fig. 4). Although all three types of C.A.Rho family proteins induced sarcomere organization and cellular hypertrophy, C.A. Cdc42-overexpressed cardiomyocytes showed significant increase in the length/width ratio that mimics the LIF-treated cardiomyocytes, while neither C.A.RhoA nor C.A.Rac1 affected the length/width ratio (Figs. 1 and 4).

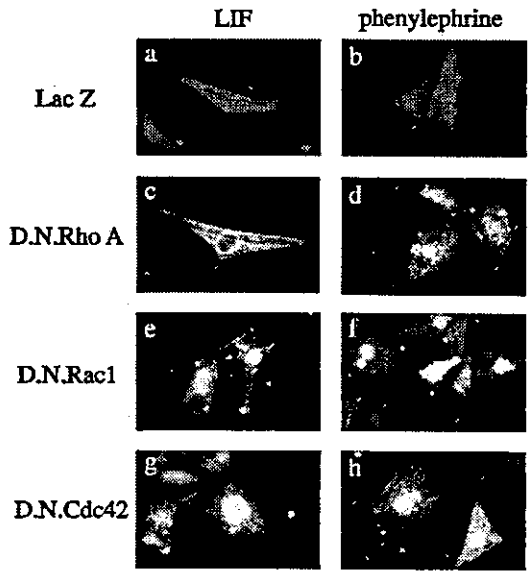

Fig. 3. Effects of dominant negative Rho family proteins on LIF- or PE-induced sarcomeric organization in cardiomyocytes. Cardiomyocytes were infected with adenovirus construct encoding LacZ (a, b), D.N.RhoA (c, d), D.N.Rac1 (e, f), or D.N.Cdc42 (g, h) for 1 h followed by treating with either 10^{-9} M LIF (a, c, e, g) or 10^{-5} M PE (b, d, f, h) for 48 h. Cardiomyocytes were stained with anti-myc monoclonal antibody (9E10) followed by FITC-conjugated anti-mouse immunoglobulin (green) and TRITC-labeled phalloidin for actin (red).

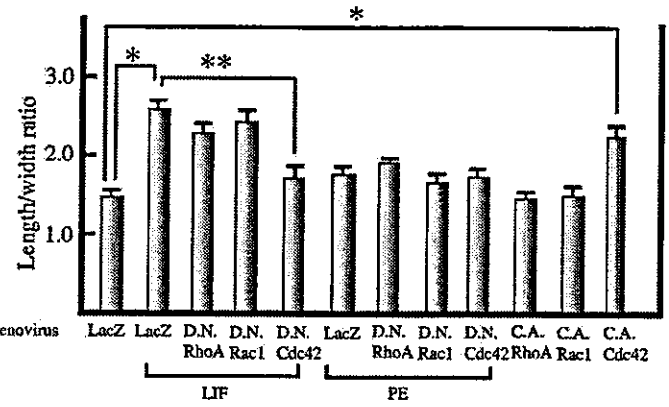

Fig. 4. Quantitative analysis of effects of mutant forms of Rho family proteins on the cell-length/width ratio in cardiomyocytes. Cardiomyocytes were infected with adenovirus construct and treated with either 10^{-9} M LIF or 10^{-5} M PE as described in the legend of Fig. 2. The effect of D.N.RhoA, D.N.Rac1, or D.N.Cdc42 on LIF or PE-induced cardiac hypertrophy and the effect of C.A.RhoA, C.A.Rac1, and C.A.Cdc42 were quantitatively analyzed by measuring cell-length/width ratio. In each experiment, over 100 cardiomyocytes were estimated and results are from three independent experiments (means ± SE). $^{*}p < 0.05$ vs control and $^{**}p < 0.05$ vs control treated with LIF.

The small GTP-binding proteins of Rho family have been demonstrated to play pivotal roles in various cytoskeletal functions such as cell shape, adhesion, and motility in various types of cells [16–19]. In cultured cardiomyocytes, we have reported that RhoA and Rac1 play critical roles in mechanical stress-induced hypertrophic responses [20]. Several groups have reported that RhoA and Rac1 are required for AngII- and PE-induced myofibrillogenesis [11,12], but the role of Cdc42 in sarcomere assembly was unclear. Overexpression of C.A. forms of RhoA, Rac1, and Cdc42 induced sarcomeric organization in cultured neonatal rat ventricular myocytes, and D.N.RhoA, Rac1, and Cdc42 inhibited LIF- and PE-induced myofibril organization. These results suggest that Cdc42 as well as RhoA and Rac1 play an important role in sarcomere organization of cardiac myocytes.

LIF, a member of IL-6 superfamily, activates the JAK-STAT signaling pathway through a common receptor gp130. Although LIF induces cardiomyocyte hypertrophy as well as PE and AngII, the shape of LIF-treated cells was quite different from that of PE-treated cells [4,5]. LIF induced assembly of sarcomeric units in series, rather than in parallel as seen after activation of G-protein-coupled receptors by PE, AngII, or endothelin-1 [7]. Myocytes from the heart with eccentric hypertrophy that is often induced by volume overload display assembly of sarcomeric units in series, while myocytes from pressure overload-induced concentric hypertrophy show parallel assembly of sarcomeric units [18–20]. Although RhoA or Rac1 has been reported to be required for AngII- or PE-induced parallel sarcomeric organization [11,12], the signaling pathway leading to this morphological difference was unknown. In the present study, C.A.Cdc42 promoted myofibril assembly in series rather than in parallel. However, neither C.A.RhoA nor C.A.Rac1 induced cell elongation. Furthermore although D.N.RhoA or D.N.Rac1 had no effect on LIF-induced cell elongation, D.N.Cdc42 inhibited LIF-induced sarcomere organization in series. These results suggest that only Cdc42 is critically involved in LIF-induced sarcomere assembly in series, although it remains to be determined whether LIF activates Cdc42 in cardiomyocytes. It has been reported that Cdc42 plays an important role in cell–cell adhesion with cadherin and β-catenin system at intercalated discs of cardiomyocytes [21,22], and that sarcomeric organization begins at intercalated discs in vitro and in vivo [23,24]. Therefore, Cdc42 may induce myofibril assembly in series by regulating the cell–cell adhesion system. Further studies are necessary to elucidate the molecular mechanism of how Cdc42 induces sarcomere assembly in series.

References

[1] S.M. LoRusso, D. Rhee, J.M. Sanger, J.W. Sanger, Premyofibril and myofibrillogenesis, Cell Motil. Cytoskeleton 28 (1994) 1–24.
[2] J.J. Hunter, K.R. Chien, Signaling pathways for cardiac hypertrophy and failure, New Engl. J. Med. 341 (1999) 1276–1283.
[3] T. Yamazaki, I. Komuro, Y. Yazaki, Molecular mechanism of cardiac cellular hypertrophy by mechanical stress, J. Mol. Cell Cardiol. 27 (1995) 133–140.
[4] K.L. King, J. Winer, D.M. Phillips, J. Quach, P.M. Williams, J.P. Mather, Phenylephrine, endothelin prostaglandin F2α′ and leukemia inhibitory factor induce different cardiac hypertrophy phenotypes in vitro, Endocrine 9 (1998) 45–55.
[5] K.C. Wollert, T. Taga, M. Saito, M. Narazaki, T. Kishimoto, C.C. Glembotski, A.B. Vernallis, J.K. Heath, D. Pennica, W.I. Wood, K.R. Chien, Cardiotrophin-1 activates a distinct form of cardiac muscle cell hypertrophy. Assembly of sarcomeric units in series VIA gp 130/leukemia inhibitory factor receptor-dependent pathways, J. Biol. Chem. 271 (1996) 9535–9545.

[6] C. Marcus, M.A. Schaub, B.A. Hefti, A. Beatrice, Various stimuli induce distinct phenotypes in cardiomycyte, J. Mol. Med. 75 (1997) 901–920.
[7] M.C. Subauste, M. vo Herrath, V. Benar, C.E. Chamberlain, T.H. Chuang, K. Chu, G.M. Bokoch, K.M. Hahn, Rho family proteins modulate rapid apoptosis induced by cytotoxic T lymphocytes and Fas, J. Biol. Chem. 275 (2000) 9725–9733.
[8] K. Nishida, Y. Kaziro, T. Satoh, Anti-apoptotic function of Rac in hematopoietic cell, Oncogene 18 (1999) 407–415.
[9] C.E. Bazenet, M.A. Mota, L.L. Rubin, The small GTP-binding protein Cdc is require of nerve growth factor withdrawal-induce neuronal death, Proc. Nat. Acad. Sci. USA 95 (1998) 3984–3989.
[10] H. Aoki, S. Izumo, J. Sadoshima, AngiotensinII activates RhoA in cardiac myocytes: a critical role of RhoA in angiotensinII-induced premyofibril formation, Cric. Res. 82 (1998) 666–676.
[11] M. Hoshijima, V.P. Sah, Y. Wang, K.R. Chien, J.H. Brown, The low molecular weight GTPase Rho regulates myofibril formation and organization in neonatal rat ventricular myocytes. Involvement of Rho kinase, J. Biol. Chem. 273 (1998) 7725–7730.
[12] J.B. Pracyk, K. Tanaka, D.D. Hegland, K.S. Kim, R. Sethi, I.I. Rovira, D.R. Blazina, L. Lee, J.T. Bruder, I. Kovesdi, P.J. Goldshmidt-Clermont, K. Irani, T. Finkel, A requirement for the rac1 GTPase in the signal transduction pathway leading to cardiac myocyte hypertrophy, J. Clin. Invest. 102 (1998) 929–937.
[13] I. Komuro, T. Kaida, Y. Shibazaki, M. Kurabayashi, F. Takaku, Y. Yazaki, Stretching cardiac myocytes stimulates proto-oncogene expression, J. Biol. Chem. 265 (1990) 3595–3598.
[14] H.R. Scholer, R. Balling, A.K. Hatzopoulos, N. Suzuki, P. Gruss, Octamer binding proteins confer transcriptional activity in early mouse embryogenesis, EMBO J. 8 (1989) 2551–2557.
[15] Y. Zhou, A. Yao, W. Zhu, S. Kudoh, Y. Hiroi, M. Shiojima, H. Uozumi, O. Kohmoto, T. Takahashi, F. Shibasaki, R. Nagai, Y. Yazaki, I. Komuro, Isoproterenol activates extracellular signal-regulated protein kinases in cardiomyocytes through calcineurin, Circulation 104 (2001) 102–108.
[16] E.E. Evers, G.C. Zondag, A. Malliri, L.S. Price, J.P. ten Klooster, R.A. van der Kammen, J.G. Collared, Rho family proteins in cell adhesion and cell migration, Eur. J. Cancer 36 (2000) 1269–1274.
[17] G.M. Bokoch, Regulation of cell function by Rho family GTPases, Immunol. Res. 21 (2000) 139–148.
[18] M. Symons, Rho family GTPases: the cytoskeleton and beyond, Trends Biochem. Sci. 21 (1996) 178–181.
[19] S. Narumiya, The small GTPase Rho: cellular functions and signal transduction, J. Biochem. 120 (1996) 215–228.
[20] R. Aikawa, I. Komuro, T. Yamazaki, Y. Zou, S. Kudoh, W. Zhu, T. Kadowaki, Y. Yazaki, Rho family small proteins play critical roles in mechanical stress-induced hypertrophic response in cardiac myocytes, Circ. Res. 84 (1999) 458–466.
[21] K. Takaishi, T. Sasaki, H. Kotani, H. Nishioka, Y. Takai, Regulation of cell–cell adhesion by Rac and Rho small G proteins in MDCK cells, J. Cell Biol. 139 (1997) 1047–1059.
[22] A. Kodama, K. Takaishi, K. Nakano, H. Nishioka, Y. Takai, Involvement of Cdc42 small G protein in cell–cell adhesion, migration, and shape of MDCK cells, Oncogene 18 (1999) 3996–4006.
[23] M.E. Eppenberger, I. Hauser, T. Baechi, M.C. Schaub, U.T. Brunner, C.A. Dechesne, H.M. Eppenberger, Immunocytochemical analysis of the regeneration of myofibrils in long-term cultures of adult cardiomyocytes of the rat, Dev. Biol. 130 (1988) 1–15.
[24] I. Klein, M. daood, T. Whiteside, Development of heart cells in culture: studies using an affinity purified antibody to a myosin light chain, J. Cell Physiol. 124 (1985) 49–53.

0022-3565/03/3041-284–293$7.00
THE JOURNAL OF PHARMACOLOGY AND EXPERIMENTAL THERAPEUTICS

JPET 304:284–293, 2003

Vol. 304, No. 1
39024/1032441
Printed in U.S.A.

Attenuation of Ischemia/Reperfusion-Induced Renal Injury in Mice Deficient in Na^+/Ca^{2+} Exchanger

JUNJI YAMASHITA, SATOMI KITA, TAKAHIRO IWAMOTO, MASAYA OGATA, MASANORI TAKAOKA, NAOKO TAZAWA, MITSUNORI NISHIKAWA, KOJI WAKIMOTO, MUNEKAZU SHIGEKAWA, ISSEI KOMURO, and YASUO MATSUMURA

Department of Pharmacology, Osaka University of Pharmaceutical Sciences, Osaka, Japan (J. Y., M. O., M. T., N. T., M. N., Y. M.); Department of Molecular Physiology, National Cardiovascular Center Research Institute, Osaka, Japan (S.K., T.I., M.S.); Discovery Research Laboratory, Tanabe Seiyaku Co. Ltd., Osaka, Japan (K.W.); and Third Department of Internal Medicine, Chiba University School of Medicine, Chiba, Japan (I.K.)

Received May 15, 2002; accepted October 1, 2002

ABSTRACT

Using Na^+/Ca^{2+} exchanger (NCX1)-deficient mice, the pathophysiological role of Ca^{2+} overload via the reverse mode of NCX1 in ischemia/reperfusion-induced renal injury was investigated. Because $NCX1^{-/-}$ homozygous mice die of heart failure before birth, we used $NCX1^{+/-}$ heterozygous mice. NCX1 protein in the kidney of heterozygous mice decreased to about half of that of wild-type mice. Expression of NCX1 protein in the tubular epithelial cells and Ca^{2+} influx via NCX1 in renal tubules were markedly attenuated in the heterozygous mice. Ischemia/reperfusion-induced renal dysfunction in heterozygous mice was significantly attenuated compared with cases in wild-type mice. Histological renal damage such as tubular necrosis and proteinaceous casts in tubuli in heterozygous mice were much less than that in wild-type mice. Ca^{2+} deposition in necrotic tubular epithelium was observed more markedly in wild-type than in heterozygous mice. Increases in renal endothelin-1 content were greater in wild-type than in heterozygous mice, and this reflected the difference in immunohistochemical endothelin-1 localization in necrotic tubular epithelium. When the preischemic treatment with KB-R7943 was performed, the renal functional parameters of both $NCX1^{+/+}$ and $NCX1^{+/-}$ acute renal failure mice were improved to the same level. These findings strongly support the view that Ca^{2+} overload via the reverse mode of Na^+/Ca^{2+} exchange, followed by renal endothelin-1 overproduction, plays an important role in the pathogenesis of ischemia/reperfusion-induced renal injury.

Renal ischemia is characterized by the depletion of ATP and the development of intracellular acidosis, which alter cellular ionic homeostasis. In particular, elevated intracellular Ca^{2+} concentration causes cellular injury during ischemia and leads to irreversible renal damage during reperfusion (Schrier et al., 1987). An increase in the intracellular Na^+ concentration has been shown to correlate with Ca^{2+} overload. The accumulation of intracellular Na^+ concentration, which is caused by inhibition of the Na^+/K^+ ATPase activity because of decreased ATP production (Cross et al., 1995) and activation of the Na^+/H^+ exchange because of intracellular acidosis (Scholz et al., 1993), has been shown to activate the Na^+/Ca^{2+} exchanger (NCX1) and subsequently to cause Ca^{2+} overload. Therefore, the NCX1 plays a crucial role in cellular injury during ischemia and in cell death during reperfusion. In the last decade, the NCX1 has been cloned and the structure/function relationship intensively studied. In addition, many investigators have studied the pathophysiological significance of NCX1 in the abnormality of the circulatory system (Philipson and Nicoll, 2000).

The role of NCX1 in ischemia/reperfusion injury has been demonstrated using the selective NCX1 inhibitor KB-R7943. This compound has been reported to be a selective and potent inhibitor of the Ca^{2+} influx mode of Na^+/Ca^{2+} exchange in cardiomyocytes, smooth muscle cells, and NCX1-transfected fibroblasts (Iwamoto et al., 1996). Similar inhibitory effects of KB-R7943 on the reverse mode of NCX1 were observed in

This work was supported by Grant-in-Aid for Scientific Research 12670098 (to Y.M.) and 12670102 (to T.I.) from the Ministry of Education, Science and Culture of Japan, and a Grant from the Cardiovascular Research Foundation (to T.I.).
Article, publication date, and citation information can be found at http://jpet.aspetjournals.org.
DOI: 10.1124/jpet.102.039024.

ABBREVIATIONS: NCX1, Na^+/Ca^{2+} exchanger; KB-R7943, 2-[2-[4-(4-nitrobenzyloxy)phenyl]ethyl]isothiourea methanesulfonate; ARF, acute renal failure; ET-1, endothelin-1; PBS, phosphate-buffered saline; BUN, blood urea nitrogen; Uosm, urinary osmolarity; FENa, fractional excretion of sodium; Ccr, creatinine clearance; KHB, Krebs-Henseleit buffer; $[Ca^{2+}]_i$, intracellular calcium concentration; BSS, balanced salt solution; $[Ca^{2+}]_o$, extracellular calcium concentration; RIA, radioimmunoassay; DMEM, Dulbecco's modified Eagle's medium; LDH, lactate dehydrogenase; Pcr, plasma creatinine concentration; UF, urine flow; SK&F96365, 1-[-[3-(4-methoxyphenyl)propoxy]-4-methoxyphenyl]-1*H*-imidazole hydrochloride; ABT-627, [2*R*-(4-methoxyphenyl)-4*S*-(1,3-benzodioxol-5-yl)-1-(*N*,*N*-di(*n*-butyl)aminocarbonyl-methyl)-pyrrolidine-3*R*-carboxylic acid]; A-192621, [2*R*-(4-propoxyphenyl)-4*S*-(1,3-benzodioxol-5-yl)-1-(*N*-(2,6-diethylphenyl)aminocarbonyl-methyl)-pyrrolidine-3*R*-carboxylic acid].

guinea pig cardiac ventricular cells (Watano et al., 1996). Furthermore, KB-R7943 efficiently improved the ischemia/reperfusion-induced injury both in isolated rat perfused heart and in anesthetized rat heart, thereby suggesting that a selective Na^+/Ca^{2+} exchange inhibitor has beneficial effects against myocardial ischemia/reperfusion injury (Nakamura et al., 1998; Ladilov et al., 1999). In the kidney, we first demonstrated the protective effects of KB-R7943 on ischemia/reperfusion-induced acute renal failure (ARF), and therefore suggested that Ca^{2+} overload via the reverse mode of NCX1 plays an important role in the pathogenesis of this renal disease (Yamashita et al., 2001).

Endothelin-1 (ET-1) is a potent vasoconstrictor peptide (Yanagisawa et al., 1988) that has been implicated as a mediator of cardiac, vascular, and renal diseases associated with regional and systemic vasoconstriction (Rubanyi and Polokoff, 1994). This peptide is produced in various tissues, including endothelial cells, smooth muscle cells, and renal tubular epithelial cells and acts through activation of G protein-coupled ET_A and ET_B receptors (Rubanyi and Polokoff, 1994). A potential contribution of ET-1 to the pathology of ischemic ARF has been suggested based on findings indicating that renal ET-1 mRNA expression, ET-1 content, and its affinity for ET receptors are elevated in the postischemic kidney (Firth and Ratcliffe, 1992; Wilhelm et al., 1999). ET_A-selective or nonselective ET_A/ET_B-receptor antagonists and ET-converting enzyme inhibitors are known to attenuate the ischemia/reperfusion-induced impairment of renal function (Gellai et al., 1995; Kuro et al., 2000; Matsumura et al., 2000). Taken together, it seems likely that renal ET-1 overproduction and its ET_A receptor-mediated actions are closely related to the pathogenesis of ischemic ARF.

The purpose of this study was to determine the pathological role of Na^+/Ca^{2+} exchange in the ischemia/reperfusion-induced ARF, using recently produced NCX1-deficient mice (Wakimoto et al., 2000). Homozygous NCX1-deficient mice ($NCX1^{-/-}$) died between embryonic days 9 and 10 (Wakimoto et al., 2000). Their hearts did not beat and cardiac myocytes showed apoptosis. Therefore, we used $NCX1^{+/-}$ heterozygous mice, which were subjected to the renal ischemia followed by reperfusion, and impairment of renal function, histological damage, and changes in renal ET-1 content were compared with those in $NCX1^{+/+}$ wild-type mice. We report here that $NCX1^{+/-}$ heterozygous mice exhibit an attenuated ischemia/reperfusion-induced renal dysfunction and cell injury, and a lowered ET-1 overproduction in the postischemic kidney, indicating that the Na^+/Ca^{2+} exchange mechanism and renal ET-1 system play an important role in the pathogenesis of postischemic ARF.

Materials and Methods

Animals. The generation of the NCX1-knockout mice has been described in detail previously (Wakimoto et al., 2000). Briefly, we cloned the NCX1 gene from a 129/SV mouse genomic library. The targeting vector was constructed by insertion of the neo cassette into the 3-kilobase pair *XbaI-XhoI* fragment containing exon 2 of NCX1 gene. The diphtheria toxin-A fragment gene was ligated to the 3′ position of the targeting vector for negative selection. The A3-1 embryonic stem cell line was transfected with the linearized targeting vector by electroporation. After G418 selection, homologous recombinants were identified by polymerase chain reaction and confirmed by Southern blot hybridization. Targeted embryonic stem cells were aggregated with eight cells from C57BL/6J (B6) mice, and chimeric blastocysts were implanted into the uterus of pseudopregnant ICR mice. Chimeric male mice were then mated to female B6 mice to confirm the germline transmission.

Surgery and Experimental Design. Male B6 mice ($NCX1^{+/-}$ and $NCX1^{+/+}$ mice; 15–20 g) were housed in a light-controlled room with a 12-h light/dark cycle, and access to food and water was ad libitum. Experimental protocols and animal care methods in the experiments were approved by the Experimental Animal Research Committee at Osaka University of Pharmaceutical Sciences. Two weeks before the study, the right kidney was removed through a small flank incision made after pentobarbital anesthesia (50 mg/kg i.p.). After a 2-week recovery period, to induce ischemic ARF, these mice were anesthetized with pentobarbital (50 mg/kg i.p.), and the left kidney was exposed through a small flank incision. The left renal artery and vein were occluded for 45 min with a nontraumatic clamp. At the end of the ischemic period, the clamp was released and blood reperfused. In some animals, KB-R7943 (10 mg/kg) or its vehicle (a mixture of 15% ethanol, 15% polyethylene glycol 400, and 70% saline) was administered as a slow bolus injection at 1 ml/kg into the external jugular vein, 5 min before the occlusion.

In sham-operated control animals, the left kidney was treated identically, except for clamping. Animals exposed to 45-min ischemia were housed in metabolic cages at 24 h after reperfusion; 24-h urine samples were taken and blood samples were drawn from the aorta at the end of urine collection period. The plasma was separated by centrifugation. These samples were used for measurements of renal functional parameters. The kidneys were excised and examined using a light microscope.

In separate experiments, left kidneys were obtained 24 h after reperfusion to determine NCX1 protein expression and ET-1 content.

Western Blotting. Tissue homogenate preparation, SDS-polyacrylamide gel electrophoresis, and immunoblotting were performed as described previously (Yamashita et al., 2001). Immunoblot analysis was performed with anti-NCX1 polyclonal antibody at 1:300 dilution with PBS (Iwamoto et al., 1998). Protein was measured with the bicinchoninic acid assay reagent (Pierce Chemical, Rockford, IL). The immunoblots were visualized using the enhanced chemiluminescence detection system (Amersham Biosciences, Inc., Piscataway, NJ).

Blood and Urine Measurements. Blood urea nitrogen (BUN) and creatinine levels in plasma and urine were determined using commercial kits, the BUN-test-Wako and Creatinine-test-Wako (Wako Pure Chemicals, Osaka, Japan), respectively. Urinary osmolality (Uosm) was measured by freezing point depression (Fiske, MA). Urine and plasma sodium concentrations were determined using a flame photometer (205D; Hitachi, Hitachinaka, Japan). Fractional excretion of sodium (FENa, %) was calculated from the formula $FENa = UNaV/(PNa \times Ccr) \times 100$, where UNaV is urinary excretion of sodium, PNa is the plasma sodium concentration, and Ccr is creatinine clearance.

Histological Studies. Histological studies were done as described previously (Yamashita et al., 2001). Histopathological changes were analyzed for tubular necrosis and proteinaceous casts, as suggested by Solez et al. (1974). Tubular necrosis and proteinaceous casts were graded as follows: no damage (− or 0), mild (± or 1, unicellular, patchy isolated damage), moderate (+ or 2, damage less than 25%), severe (++ or 3, damage between 25 and 50%), and very severe (+++ or 4, more than 50% damage). Evaluations were made in a blind manner.

Using von Kossa method, the amount of black reaction products indicated as Ca^{2+} deposition in necrotic tubular epithelium was also determined by microscopic observation.

Primary Culture of Proximal and Distal Tubular Cells. Proximal and distal tubular cells were prepared from $NCX1^{+/+}$ and $NCX1^{+/-}$ mice with a modification of methods described previously (Gesek et al., 1987). Briefly, mice were anesthetized with sodium pentobarbital (50 mg/kg i.p.) and the left kidney was perfused with ice-cold modified Krebs-Henseleit buffer (KHB) through the thoracic aorta after ligation of the aorta and vena cava above the renal

vessels. Modified KHB contains the following: 118 mM NaCl, 4.0 mM KCl, 1.0 mM KH_2PO_4, 27.2 mM $NaHCO_3$, 1.25 mM $CaCl_2$, 1.20 mM $MgCl_2$, 5.0 mM glucose, and 10 mM HEPES. The kidney was removed and the cortex was cut into 1-mm-thick slices, being incubated for 40 min at 37°C in atmosphere of 95% O_2/5% CO_2. The slices were then washed with KHB and transferred to an ice-cold solution. Nephron segments were isolated from the cortex region under microscope. Proximal tubules (segments 1–3) just after the glomerulus and distal convoluted tubules just after the thick ascending limb were excised. These isolated tubules were then explanted for 4 to 5 days on 35-mm dishes in Dulbecco's modified Eagle's medium supplemented with 10% heat-inactivated fetal calf serum, 100 U/ml penicillin, and 100 μg/ml streptomycin.

Measurement of $[Ca^{2+}]_i$ in Proximal and Distal Tubular Cells. $[Ca^{2+}]_i$ was monitored using Fluo-3/acetoxymethyl ester as a fluorescent Ca^{2+} indicator. Cells in 35-mm dishes were loaded with 4 μM Fluo-3/acetoxymethyl ester for 40 min at 37°C in 1 ml of balanced salt solution [BSS; 10 mM HEPES-Tris (pH 7.4), 146 mM NaCl, 4 mM KCl, 2 mM $MgCl_2$, 1 mM $CaCl_2$, and 10 mM glucose]. Loaded cells were then washed twice with BSS. Cells were exposed to Ca^{2+}, Mg^{2+}-free BSS containing 0.2 mM EGTA for 10 min and then to BSS containing 2 mM Ca^{2+}. KB-R7943 (10 μM) was pretreated for 10 min before the repletion of $[Ca^{2+}]_o$. Fluorescence signals from single tubular cells with excitation at 488 nm were monitored by confocal laser scanning microscope system (MRC1024; Bio-Rad, Hercules, CA). The fluorescence intensity of individual cells (F) was normalized to that (F_0) before adding 2 mM Ca^{2+}.

Renal ET-1 Assay. ET-1 was extracted from the kidney, as described elsewhere (Fujita et al., 1995). Briefly, kidneys were weighed and homogenized for 60 s in 8 ml of ice-cold organic solution (chloroform/methanol, 2:1, including 1 mM *N*-ethylmaleimide). The homogenates were left overnight at 4°C and then 0.4 ml of distilled water was added after which the homogenates were centrifuged at 1500*g* for 30 min and the resultant supernatant was stored. Aliquots of the supernatant were diluted 1/10 with a 0.09% trifluoroacetic acid solution and applied to Sep-Pak C18 cartridges. The sample was eluted with 3 ml of 63.3% acetonitrile and 0.1% trifluoroacetic acid in water. Eluates were dried in a centrifugal concentrator and the dried residue was reconstituted in assay buffer for radioimmunoassay (RIA). The clear solution was subjected to RIA. The recovery of ET-1 was approximately 80%. RIA for tissue ET-1 was done, as described previously (Matsumura et al., 1990b).

Immunohistochemistry. Excised left kidneys were preserved in phosphate-buffered 10% formalin, after which the kidneys were chopped into small pieces, embedded in paraffin wax, and cut at 3 μm. Tissue sections were incubated for 30 min at 37°C with anti-ET-1 polyclonal antibody (Peptide Institute, Inc., Osaka, Japan) or with anti-NCX1 polyclonal antibody (Iwamoto et al., 1998) at 1:2000 and 1:300 dilution with PBS, respectively. After washing with PBS, the sections were further incubated with goat anti-rabbit biotinylated secondary antibody (Nichirei, Tokyo, Japan) at 37°C for 10 min and then the streptavidin-horseradish peroxidase (Nichirei) was applied for 5 min. The complex was visualized with 3,3-diamonobenzidine.

Hypoxia and Reoxygenation in LLC-PK_1. LLC-PK_1 (American Type Culture Collection, Manassas, VA), a porcine kidney cell line, was grown in Dulbecco's modified Eagle's medium (DMEM) supplemented with 10% fetal calf serum, 50 μg/ml streptomycin, and 50 U/ml penicillin at 37°C in a CO_2 incubator (95% air, 5% CO_2). When the cells cultured in 24-well plates became confluent, the culture medium was changed to DMEM without glucose and serum and the cells were exposed to the hypoxic condition using an Anaero Pack Pouch (Mitsubishi Bas Chemical Co., Inc., Tokyo, Japan), in which the oxygen concentration was less than 1% within 1 h after the exposure. After 6 h of hypoxia, the cells were put in a CO_2 incubator for 1 h in the DMEM to which glucose was added at the beginning of reoxygenation. After the exposure of the cells to hypoxia and reoxygenation, lactate dehydrogenase (LDH) activity in the culture supernatant for 7 h was measured with a commercial kit (Wako Pure Chemicals). KB-R7943 (10 μM) was added to the medium at the beginning of hypoxia and/or reoxygenation. LDH release was expressed as a percentage of total cellular LDH activity.

Statistical Analysis. Values are mean ± S.E.M. For statistical analysis, we used one-way analysis of variance followed by Bonferroni's or Dunnett's multiple comparison tests. Histological data were analyzed using the Kruskal-Wallis nonparametric test combined with the Steel-type multiple comparison test. For all comparisons, differences were considered significant at $P < 0.05$.

Results

Expression and Localization of NCX1 Protein. To justify the use of $NCX1^{+/-}$ heterozygous and $NCX1^{+/+}$ wild-type mice, NCX1 protein expression in the kidney of these animals was examined. As shown in Fig. 1, NCX1 protein level in renal tissues of $NCX1^{+/-}$ mice was about half of that seen in $NCX1^{+/+}$ mice. On the other hand, protein levels of Na^+/K^+-ATPase, sarcoplasmic reticulum Ca^{2+}-ATPase (type 2) and L-type voltage-dependent Ca^{2+} channel did not differ between $NCX1^{+/-}$ and $NCX1^{+/+}$ mice (data not shown). In addition, an immunohistochemical study clearly indicated that a staining for NCX1 protein expression was much more intense in tubular epithelial cells of renal cortex of $NCX1^{+/+}$ wild-type mice than in those of $NCX1^{+/-}$ mice (Fig. 2).

$[Ca^{2+}]_i$ Rise Evoked by the Reverse Mode of Na^+/Ca^{2+} Exchange in Cultured Renal Tubular Cells. $[Ca^{2+}]_o$ reple-

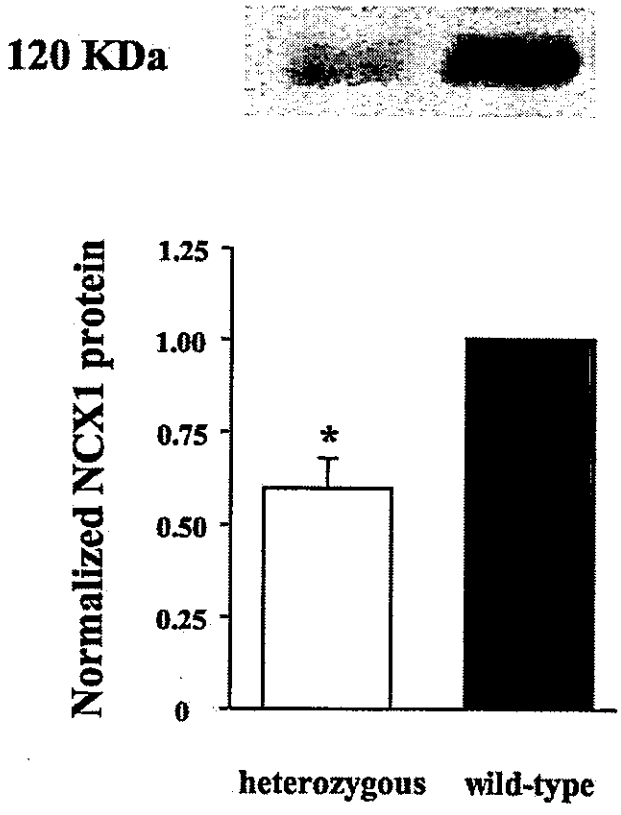

Fig. 1. NCX1 protein expression in renal tissues of $NCX1^{+/+}$ wild-type and $NCX1^{+/-}$ heterozygous mice. Each column and bar represents the mean ± S.E.M. ($n = 6$). *, $P < 0.01$, compared with wild-type mice.

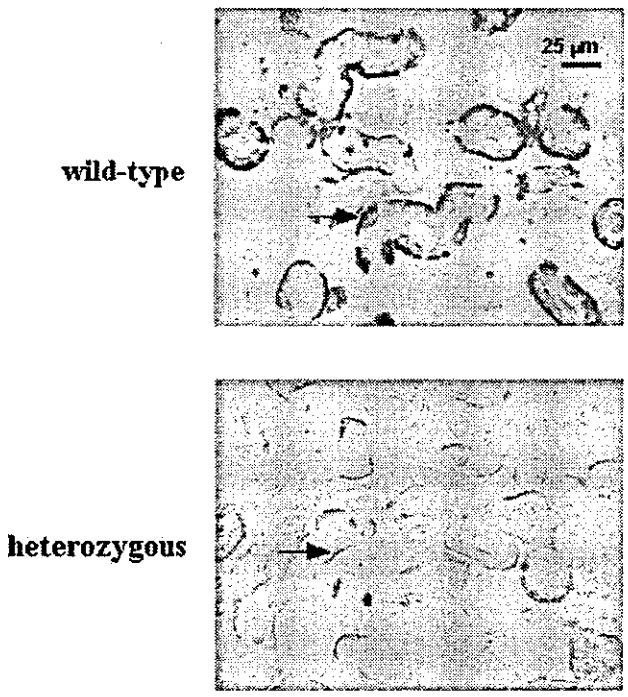

Fig. 2. Immunohistochemistry for NCX1 protein in the renal cortex of $NCX1^{+/+}$ wild-type and $NCX1^{+/-}$ heterozygous mice. Arrows indicate NCX1 protein expression in tubular epithelial cells. The protein expression was much more intense in $NCX1^{+/+}$ than in $NCX1^{+/-}$ mice.

tion after a period of $[Ca^{2+}]_o$ depletion is known to cause Ca^{2+} overloading via Na^+/Ca^{2+} exchange in cardiomyocytes or neuronal cells, a process called the Ca^{2+} paradox (Chapman and Tunstall, 1987). To assess the functional difference of Na^+/Ca^{2+} exchange in renal tubules between $NCX1^{+/+}$ and $NCX1^{+/-}$ mice, we examined $[Ca^{2+}]_i$ rise evoked by the Ca^{2+} paradox in cultured renal tubular cells using Ca^{2+} indicator Fluo-3. When distal tubular cells of $NCX1^{+/+}$ mice were exposed with a Ca^{2+}, Mg^{2+}-free buffer for 10 min and then placed in a buffer containing 2 mM Ca^{2+}, $[Ca^{2+}]_i$ markedly increased. In the proximal tubular cells, $[Ca^{2+}]_i$ rise was also observed, although being significantly smaller than that in distal tubular cells (Fig. 3). These $[Ca^{2+}]_i$ responses were blocked over 90% by pretreatment with KB-R7943 (10 μM), an inhibitor for the reverse mode of Na^+/Ca^{2+} exchange, but not significantly affected by verapamil (10 μM), L-type Ca^{2+} channel blocker, or SK&F96365 (50 μM), a blocker of store-operated Ca^{2+} channels (data not shown). In $NCX1^{+/-}$ mice, on the other hand, the $[Ca^{2+}]_i$ elevations in both tubular cells induced by 2 mM Ca^{2+} were markedly down-regulated compared with the case of $NCX1^{+/+}$ mice.

Renal Function after Ischemia/Reperfusion. As shown in Fig. 4, renal functional parameters of mice subjected to 45-min ischemia showed a marked deterioration, as measured 48 h after reperfusion. Compared with each sham-operated control animals, both $NCX1^{+/-}$ and $NCX1^{+/+}$ mice exhibited increases in BUN, plasma creatinine concentration (Pcr), urine flow (UF) and FENa, and decreases in Ccr, and Uosm. However, ischemia/reperfusion-induced changes in renal functional parameters of $NCX1^{+/-}$ mice were considerably small, compared with cases in $NCX1^{+/+}$ mice (BUN: $NCX1^{+/-}$, 78.0 ± 8.8 versus $NCX1^{+/+}$, 142.6 ± 7.4 mg/dl; Pcr, $NCX1^{+/-}$, 0.80 ± 0.10 versus $NCX1^{+/+}$, 1.34 ± 0.05 mg/dl; Ccr, $NCX1^{+/-}$, 2.15 ± 0.23 versus $NCX1^{+/+}$, 0.95 ± 0.13 ml min^{-1} kg^{-1}; UF, $NCX1^{+/-}$, 88.1 ± 10.4 versus $NCX1^{+/+}$, 102.6 ± 10.7 μl min^{-1} kg^{-1}; Uosm, $NCX1^{+/-}$, 663 ± 73 versus $NCX1^{+/+}$, 501 ± 18 mOsM/kg; FENa, $NCX1^{+/-}$, 1.05 ± 0.16 versus $NCX1^{+/+}$, 1.93 ± 0.12%). On the other hand, there were no significant differences in renal functional parameters between $NCX1^{+/+}$ and $NCX1^{+/-}$ sham-operated control mice.

Histological Renal Damage after Ischemia/Reperfusion. Histological examination revealed severe lesions in the kidney of $NCX1^{+/+}$ mice (48 h after the ischemia/reperfusion). These changes were characterized by tubular necrosis (Fig. 5b, outer zone outer stripe of medulla) and proteinaceous casts in tubuli (Fig. 5f, inner zone of medulla). In $NCX1^{+/-}$ mice, histologically evident damage was significantly less than that seen in $NCX1^{+/+}$ mice (Figs. 5, d and h; Table 1).

Ca^{2+} Deposition after Ischemia/Reperfusion. Figure 6 shows light micrographs of Ca^{2+} deposition demonstrated by von Kossa method in the kidney subjected to 45-min ischemia followed by reperfusion. Ca^{2+} deposition in medullary tubular epithelium of kidney of $NCX1^{+/+}$ mice was more evident compared with the case of $NCX1^{+/-}$ mice.

Effects of KB-R7943 on the Ischemia/Reperfusion-Induced Renal Dysfunction. To further evaluate the possible involvement of NCX1 in the ischemia/reperfusion-induced renal injury, the effect of pharmacological blockade of NCX1 was examined. As shown in Fig. 7, preischemic treatment with KB-R7943 improved the renal functional parameters of both $NCX1^{+/+}$ and $NCX1^{+/-}$ ARF mice to the same level.

Effects of KB-R7943 on the Hypoxia/Reoxygenation-Induced Injury in LLC-PK_1. LLC-PK_1 cells, derived from pig kidney, have characteristics of proximal tubules. We evaluated the effect of KB-R7943 on the hypoxia/reoxygenation-induced cell injury in LLC-PK_1. Hypoxia/reoxygenation technique is known as in vitro model system of ischemia/reperfusion-induced renal injury. As shown in Fig. 8, an enhanced LDH release from the cells exposed to hypoxia followed by reoxygenation was markedly suppressed by the treatment with KB-R7943 during the hypoxia. Similar suppressive effect of KB-R7943 was also observed by the addition at the beginning of reoxygenation.

Renal ET-1 Content after Ischemia/Reperfusion. To confirm the contribution of ET-1 to ischemia/reperfusion-induced renal injury both in $NCX1^{+/-}$ and $NCX1^{+/+}$ mice, we measured renal ET-1 content at 24 h after reperfusion. As shown in Fig. 9, renal ET-1 content was significantly increased by the ischemia/reperfusion, both in $NCX1^{+/+}$ and $NCX1^{+/-}$ mice, compared with that seen in each sham mice. However, ischemia/reperfusion-induced changes in renal ET-1 content of $NCX1^{+/-}$ mice were considerably small, compared with cases in $NCX1^{+/+}$ mice ($NCX1^{+/-}$, 0.71 ± 0.06 versus $NCX1^{+/+}$, 1.26 ± 0.23 ng/g tissue).

Immunohistochemical Analysis. To determine the localization of renal ET-1 peptide expression after the ischemia/reperfusion, an immunohistochemical study was done. As clearly indicated in Fig. 10, a staining for ET-1 peptide expression was intense in tubular lumen containing necrotic cells, and it was more prominent in $NCX1^{+/+}$ than in $NCX1^{+/-}$ mice.

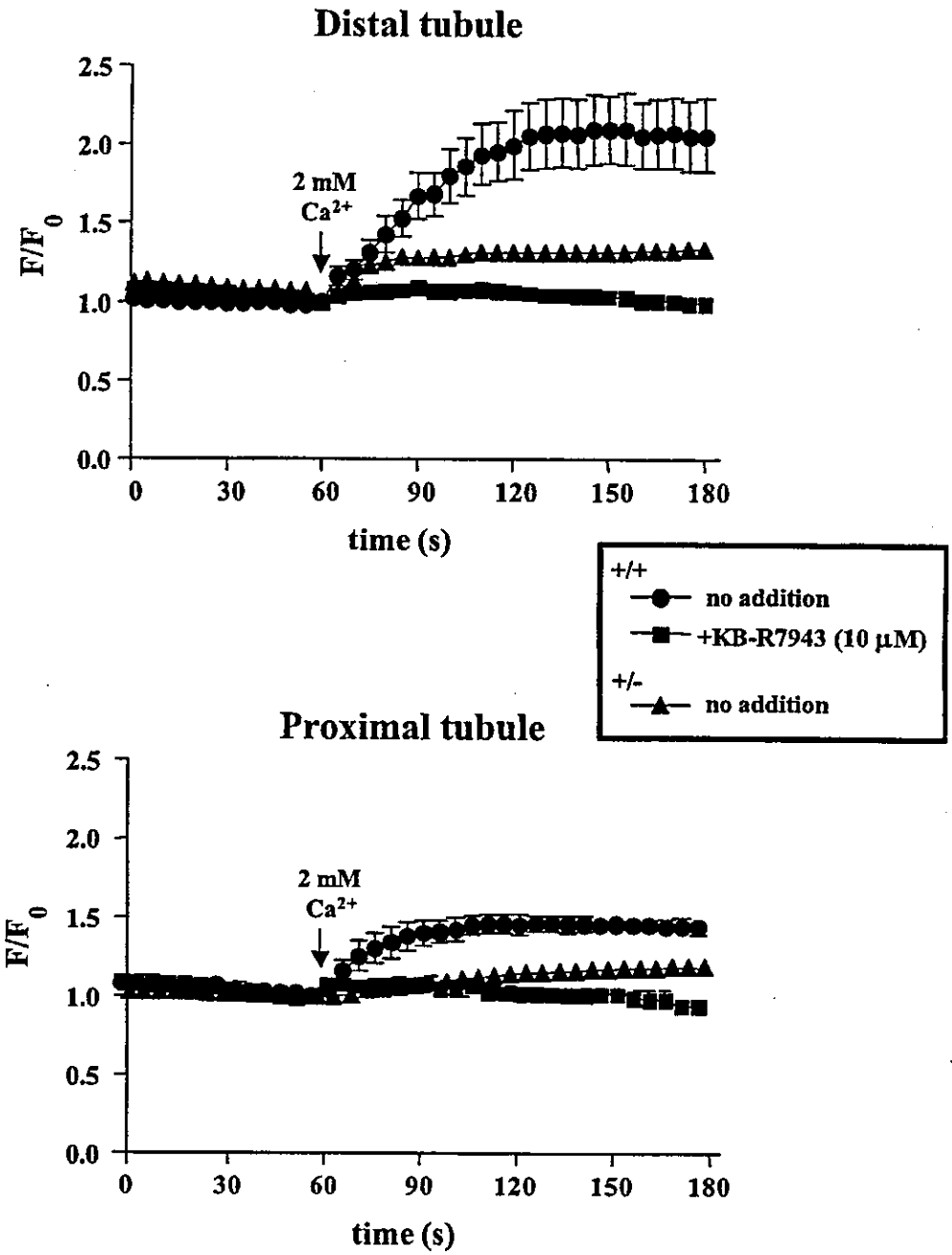

Fig. 3. $[Ca^{2+}]_i$ elevations evoked by the Ca^{2+} paradox in cultured proximal and distal tubular cells from $NCX1^{+/+}$ wild-type and $NCX1^{+/-}$ heterozygous mice. Fluo-3-loaded cells were exposed to a Ca^{2+}, Mg^{2+}-free BSS containing 0.2 mM EGTA for 10 min and then to BSS containing 2 mM Ca^{2+}, with or without 10 μM KB-R7943. KB-R7943 was pretreated for 10 min before the repletion of Ca^{2+}. The fluorescence intensity of individual cells was normalized to that (F_0) before adding 2 mM Ca^{2+}. Each point and bar represents the mean ± S.E.M.

Discussion

We investigated the pathological role of NCX1 in ischemia/reperfusion-induced renal injury using NCX1-knockout mice. Because $NCX1^{-/-}$ homozygous mice die of heart failure before birth (Wakimoto et al., 2000), we used $NCX1^{+/-}$ heterozygous mice, in which NCX1 protein expression in renal tissues was decreased to about half of those of $NCX1^{+/+}$ wild-type mice. Furthermore, expression of NCX1 protein in the tubular epithelial cells and Na^+/Ca^{2+} exchange activity of renal tubules were markedly attenuated in the heterozygous mice, thereby indicating the usefulness of these mice in examining the renal pathophysiological role of NCX1.

In the present study, the ischemia/reperfusion-induced renal dysfunction and histological damage was moderate in $NCX1^{+/-}$ mice compared with cases in $NCX1^{+/+}$ mice. His-

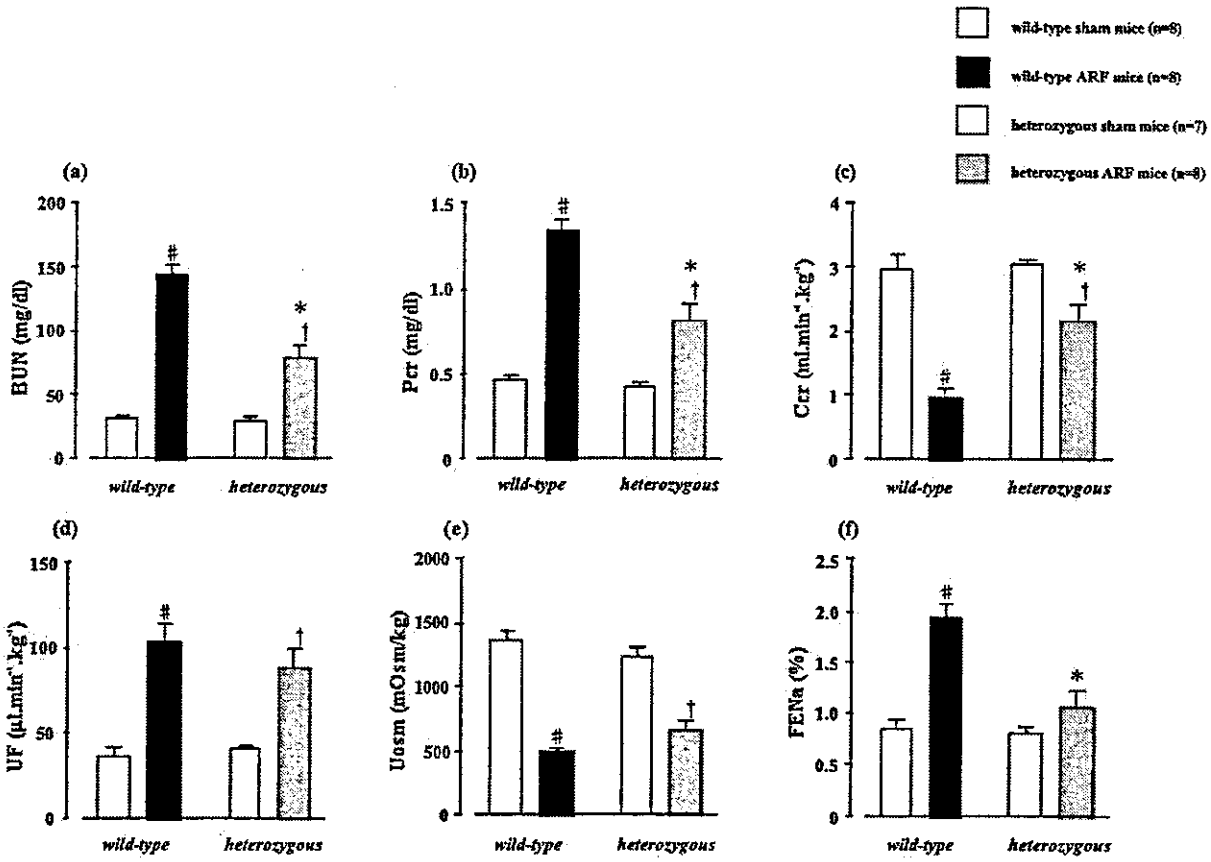

Fig. 4. Renal functional parameters of NCX1$^{+/+}$ wild-type and NCX1$^{+/-}$ heterozygous mice, with or without ARF. BUN (a), Pcr (b), Ccr (c), UF (d); Uosm (e), and FENa (f). Each column and bar represents the mean ± S.E.M. #, $P < 0.01$, compared with wild-type sham mice; †, $P < 0.01$, compared with heterozygous sham mice; *, $P < 0.01$, compared with wild-type ARF mice.

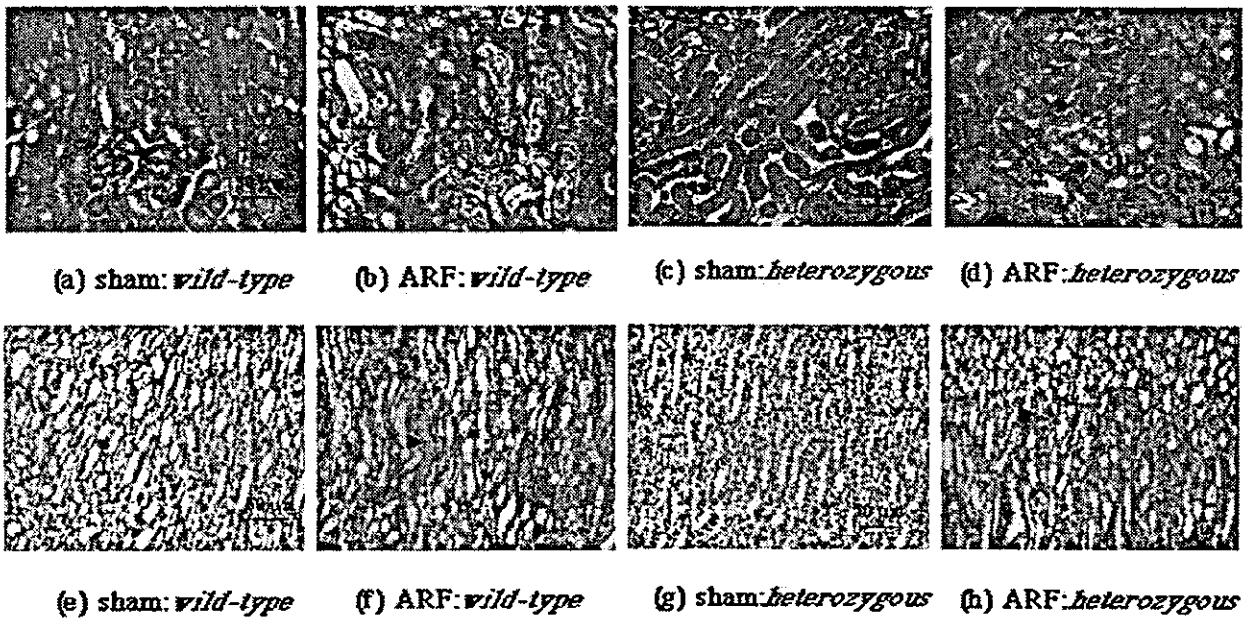

Fig. 5. Light microscopy of outer zone outer stripe of medulla (a–d) and inner zone of medulla (e–h) of the kidney of NCX1$^{+/+}$ wild-type and NCX1$^{+/-}$ heterozygous mice, with or without ARF. Arrows indicate tubular necrosis (b and d) and proteinaceous casts in tubuli (f and h) (hematoxyline and eosin staining).

TABLE 1

Histopathological changes in kidneys of wild-type and heterozygous mice, with or without ARF

Data are expressed as the number of animals with histopathological changes. Values in parentheses represent the mean ± S.E.M. of histopathological change/grade. Grades: no changes (− or 0), mild (± or 1), moderate (+ or 2), severe (++ or 3), very severe (+++ or 4).

	Wild-Type										Heterozygous									
	Sham Mice (n = 5)					ARF Mice (n = 6)					Sham Mice (n = 5)					ARF Mice (n = 6)				
Histopathological changes/grade	− (0	± 1	+ 2	++ 3	+++ 4)	− (0	± 1	+ 2	++ 3	+++ 4)	− (0	± 1	+ 2	++ 3	+++ 4)	− (0	± 1	+ 2	++ 3	+++ 4)
Tubular necrosis	5	0	0	0	0	0	0	0	4	2	5	0	0	0	0	0	3	3	0	0
								(3.33 ± 0.21[a])										(1.50 ± 0.22[b,c])		
Protein casts	5	0	0	0	0	0	0	0	2	4	5	0	0	0	0	0	2	2	2	0
								(3.67 ± 0.21[a])										(2.00 ± 0.37[b,c])		

ARF, acute renal failure.
[a] $P < 0.01$, compared with wild-type sham mice.
[b] $P < 0.01$, compared with heterozygous sham mice.
[c] $P < 0.01$, compared with wild-type ARF mice.

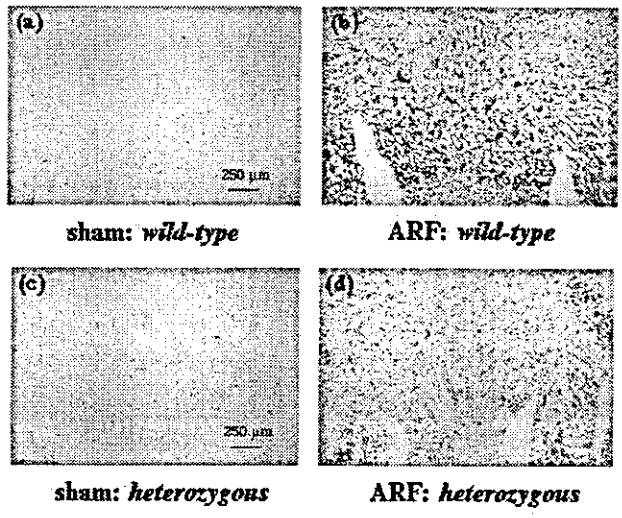

Fig. 6. Light microscopy of Ca^{2+} deposition in medulla of the kidney of $NCX1^{+/+}$ wild-type and $NCX1^{+/-}$ heterozygous mice, with or without ARF. Ca^{2+} deposition in medullary tubular epithelium of kidney of $NCX1^{+/+}$ ARF mice (b) was more evident compared with the case of $NCX1^{+/-}$ ARF mice (d) (von Kossa staining).

tochemically visualized Ca^{2+} deposition in medullary tubular epithelium of postischemic kidney of $NCX1^{+/-}$ mice was less evident than that seen in $NCX1^{+/+}$ mice. On the other hand, pharmacological blockade of NCX1 with KB-R7943 improved the renal dysfunction observed in both $NCX1^{+/+}$ and $NCX1^{+/-}$ ARF mice to the same level. An increment of ET-1 content in postischemic kidney of $NCX1^{+/-}$ mice was also less than that observed in $NCX1^{+/+}$ mice, and this difference reflected an immunohistochemical localization of ET-1 in tubular lumen-containing necrotic cells. These findings suggest that Ca^{2+} overload via the reverse mode of NCX1, followed by renal ET-1 overproduction, plays an important role in the pathogenesis of ischemia/reperfusion-induced renal injury.

In normal cardiac cells, NCX1 extrudes Ca^{2+} from sarcolemma to maintain the intracellular Ca^{2+} concentration at the diastolic level. In contrast, in ischemic cardiac cells where intracellular pH decreases, the intracellular Na^+ concentration rises through the Na^+/H^+ exchange system, which in turn increases the intracellular Ca^{2+} concentration through the Na^+/Ca^{2+} exchange system (Dennis et al., 1990). The Ca^{2+} overload via this system seems to contribute to the ischemia/reperfusion injury in the heart (Tani and Neely, 1989; Cross et al., 1998). This view may be applicable to the case of the pZostischemic ARF. Although the pathological mechanisms of Ca^{2+} overload in ischemic kidney have not been fully elucidated, there is substantial evidence indicating that increased cytosolic Ca^{2+} may be an important mediator of epithelial cell necrosis, which is a characteristic of ischemic ARF and that Ca^{2+} overload is a primary factor in certain types of cell injury (Wilson et al., 1984). In addition, a preischemic treatment with Ca^{2+} channel blockers has been known to exert a protective effect against the ischemia/reperfusion-induced renal injury (Goldfarb et al., 1983; Yamashita et al., 2001). Most recently, we found that KB-R7943, a selective and potent inhibitor of the Ca^{2+} influx mode of Na^+/Ca^{2+} exchange (Iwamoto et al., 1996; Watano et al., 1996), efficiently attenuated the ischemia/reperfusion-induced renal injury in both cases of pre- and postischemic treatments, thereby suggesting that Ca^{2+} overload via the reverse mode of the Na^+/Ca^{2+} exchange is a crucial factor in the pathology of postischemic renal insufficiency, and that an inhibitor of NCX1 may be an beneficial therapeutic agent for the postischemic ARF (Yamashita et al., 2001).

In the present study, using $NCX1^{+/-}$ heterozygous mice we confirmed the pathophysiological importance of Ca^{2+} handling via NCX1 in the ischemia/reperfusion-induced renal injury. The level of NCX1 protein expression in renal tissues of the $NCX1^{+/-}$ mice was about half of that seen in $NCX1^{+/+}$ wild-type mice. Ca^{2+} influx via Na^+/Ca^{2+} exchange, which is abolished by a selective NCX1 inhibitor KB-R7943, in proximal and distal tubular cells were much less potent in $NCX1^{+/-}$ mice than in $NCX1^{+/+}$ mice. In addition, we obtained the evidences that protein levels of Na^+/K^+-ATPase, sarcoplasmic reticulum Ca^{2+}-ATPase, and L-type voltage-dependent Ca^{2+} channel did not differ between $NCX1^{+/+}$ and $NCX1^{+/-}$ mice (T. Iwamoto, unpublished data). These findings seem to justify the usefulness of these animals in renal pathophysiological study. However, an attenuation of ischemia/reperfusion-induced renal injury observed in $NCX1^{+/-}$ mice was only partial. Thus, to elucidate more precisely the pathophysiological role of NCX1 in the postischemic ARF, further studies using $NCX1^{-/-}$ homozygous mice are needed. To attain this, adult $NCX1^{-/-}$ mice should be produced by the tissue (heart)-specific transgenic rescue. Furthermore, the rescued adult $NCX1^{-/-}$ mice may provide new information on the physiological role of NCX1 in regulatory mechanisms of renal function, although we observed no significant